VIP Polymeric Nanoparticles Very Important Paper

How to cite: *Angew. Chem. Int. Ed.* **2022,** *61,* e202113424
International Edition: doi.org/10.1002/anie.202113424
German Edition: doi.org/10.1002/ange.202113424

Transformer-Induced Metamorphosis of Polymeric Nanoparticle Shape at Room Temperature

*Kostas Parkatzidis, Nghia P. Truong, Manon Rolland, Viviane Lutz-Bueno, Emily H. Pilkington, Raffaele Mezzenga, and Athina Anastasaki**

Abstract: *Controlled polymerizations have enabled the production of nanostructured materials with different shapes, each exhibiting distinct properties. Despite the importance of shape, current morphological transformation strategies are limited in polymer scope, alter the chemical structure, require high temperatures, and are fairly tedious. Herein we present a rapid and versatile morphological transformation strategy that operates at room temperature and does not impair the chemical structure of the constituent polymers. By simply adding a molecular transformer to an aqueous dispersion of polymeric nanoparticles, a rapid evolution to the next higher-order morphology was observed, yielding a range of morphologies from a single starting material. Significantly, this approach can be applied to nanoparticles produced by disparate block copolymers obtained by various synthetic techniques including emulsion polymerization, polymerization-induced self-assembly and traditional solution self-assembly.*

Controlled radical polymerization (CRP) has been highlighted as one of the top ten emerging technologies in chemistry that could change the world, according to a recent IUPAC report.[1] Perhaps a key feature of CRP (also of ionic polymerizations) is that the vast majority of the generated polymer chains possess an active end-group which can be further exploited to form block copolymers.[2] These block copolymers can self-assemble in solution, producing core-shell polymeric nanoparticles.[3] Such nanostructures are increasingly used in a range of fields, spanning from the automotive, environment, energy, catalysis to biomedical, pharmaceutical and polymer industries.[4] Owing to these advantageous characteristics, numerous synthetic techniques for these nanoparticles have emerged including the so-called traditional self-assembly,[5] emulsion and dispersion polymerizations (e.g. polymerization-induced self-assembly (PISA))[6] and crystallization-driven self-assembly.[7] A particular focus of these strategies is to control the nanoparticle morphology from low to high order (e.g. from spheres to worms, and vesicles), as they exhibit distinct properties and performance.[8] For instance, worms present higher surface area and flexibility than spheres, spheres show higher cell uptake than worms and vesicles have the advantage of encapsulating both hydrophobic and hydrophilic compounds.[9] These distinct properties are typically acquired by using nanoparticles composed of disparate block copolymers or varied molecular weights and synthesized by different techniques.[8,10] To realize a more direct comparison among various morphologies (e.g. enable structure–property relationship studies or theoretical simulations), alternative strategies that allow the efficient transformation between different nanoparticle shapes have also been developed.[11] Additional benefits of these strategies include the use of a single block copolymer to produce polymeric nanoparticles of various shapes (i.e. rather than synthesizing block copolymers consisting of different degrees of polymerization (DPs)) and the facile identification of the conditions for morphological transformation (i.e. instead of requiring the optimization of multiple parameters to control the morphology). For instance, the addition of ions in poly(styrene-*b*-acrylic acid) nanoparticles, obtained through traditional solution self-assembly, triggered the morphological transformation into various morphologies.[11a] This transformation was induced due to decreased repulsion within the hydrophilic segments caused by the binding or bridging of the corona forming block (*e.g.* poly(acrylic acid)). In another report, poly(lauryl methacrylate-*b*-benzyl methacrylate) nanoparticles produced by PISA were shown to undergo a change in morphology by adjusting the solution temperature.[12] Such temperature-induced morphological transformations do not rely on thermo-responsive polymers but on the surface solvation of the nanoparticles.[12]

In contrast, other strategies exclusively require thermo-responsive materials to trigger such transformations.[13] Further methods include the use of external stimuli such as

[*] K. Parkatzidis, Dr. N. P. Truong, M. Rolland, Prof. Dr. R. Mezzenga, Prof. Dr. A. Anastasaki
Laboratory of Polymeric Materials
Department of Materials, ETH Zurich
Vladimir-Prelog-Weg 5, Zurich 8093 (Switzerland)
E-mail: Athina.anastasaki@mat.ethz.ch

Dr. V. Lutz-Bueno, Prof. Dr. R. Mezzenga
Department of Health Sciences and Technology
ETH Zurich
Zurich 8092, (Switzerland)

Dr. N. P. Truong, Dr. E. H. Pilkington
Monash Institute of Pharmaceutical Sciences
Monash University
Parkville, Victoria 3052 (Australia)

light, pH and chemical stimuli to aid morphological transformations.[14]

Despite these significant advances, current transformation approaches are limited in polymer scope (i.e. transformation is possible through a specific diblock copolymer rather than a range of materials), typically require a significant temperature change which may be incompatible with certain applications (e.g. $T > 50\,^{\circ}C$ may prevent drug encapsulation), may alter the chemical structure among different shapes through either demanding chemical modifications or the use of stimuli such as pH and light, and can be fairly tedious and time-consuming (i.e. transformation is completed in hours).[11c,15]

Herein we present a simple and fast methodology that allows for a rapid and efficient transformer-induced metamorphosis (TIM) of polymeric nanoparticles through the addition of small organic molecules, referred in this work as transformers. This methodology does not change the molecular weight or chemical structure of the polymers, operates at room temperature, and is applicable to a range of block copolymers and synthetic techniques (Figure 1).

First, we synthesized spherical particles by aqueous reversible addition-fragmentation chain-transfer polymerization (RAFT) emulsion polymerization of styrene utilizing poly(di(ethylene glycol) ethyl ether methacrylate-*co*-*N*-(2-hydroxypropyl) methacrylamide) (P(DEGMA-*co*-HPMA)) ($M_n = 8600$, Figure S1) as the macromolecular chain transfer agent (macro-CTA). This macro-CTA was synthesized through an adapted RAFT-mediated solution polymerization protocol.[16] It is noted that this macro-CTA is a thermo-responsive polymer that can form aggregates at 70 °C (Table S1). The emulsion polymerization was commenced at 70 °C yielding a well-defined diblock copolymer P((DEGMA-*co*-HPMA)-*b*-styrene) ($M_n = 14300$, Figure S2). The unreacted styrene was then evaporated and the solution was cooled down at room temperature (Figures S3 & S4). Using transmission electron microscopy (TEM) analysis, spherical aggregates ($\approx$1200 nm) were observed and their spherical morphology maintained intact for several months (Figure S5). Interestingly, when a small amount of a molecular transformer (i.e. toluene, 5 $\mu L\,mL^{-1}$) was added, at room temperature, a turbidity change was immediately noticed upon mildly shaking the solution for approximately 5 seconds (Figure 2d). Subsequent TEM analysis revealed a change from the initial spherical aggregates to wormballs (Figure 2b). This interesting morphology suggests that acquiring worm-like nanoparticles may also be possible. Indeed, by further increasing the amount of the injected transformer (additional 10 $\mu L\,mL^{-1}$), worm-like nanoparticles could be obtained as confirmed by TEM, while accompanied by a further change in turbidity (Figure 2d). It is also noted that at room temperature, and in the presence of added toluene, the original macro-CTA is water-soluble, thus forming the corona while polystyrene (PS) is water-insoluble and therefore becoming the core. Our current hypothesis is that the transformer (i.e. toluene, which has a

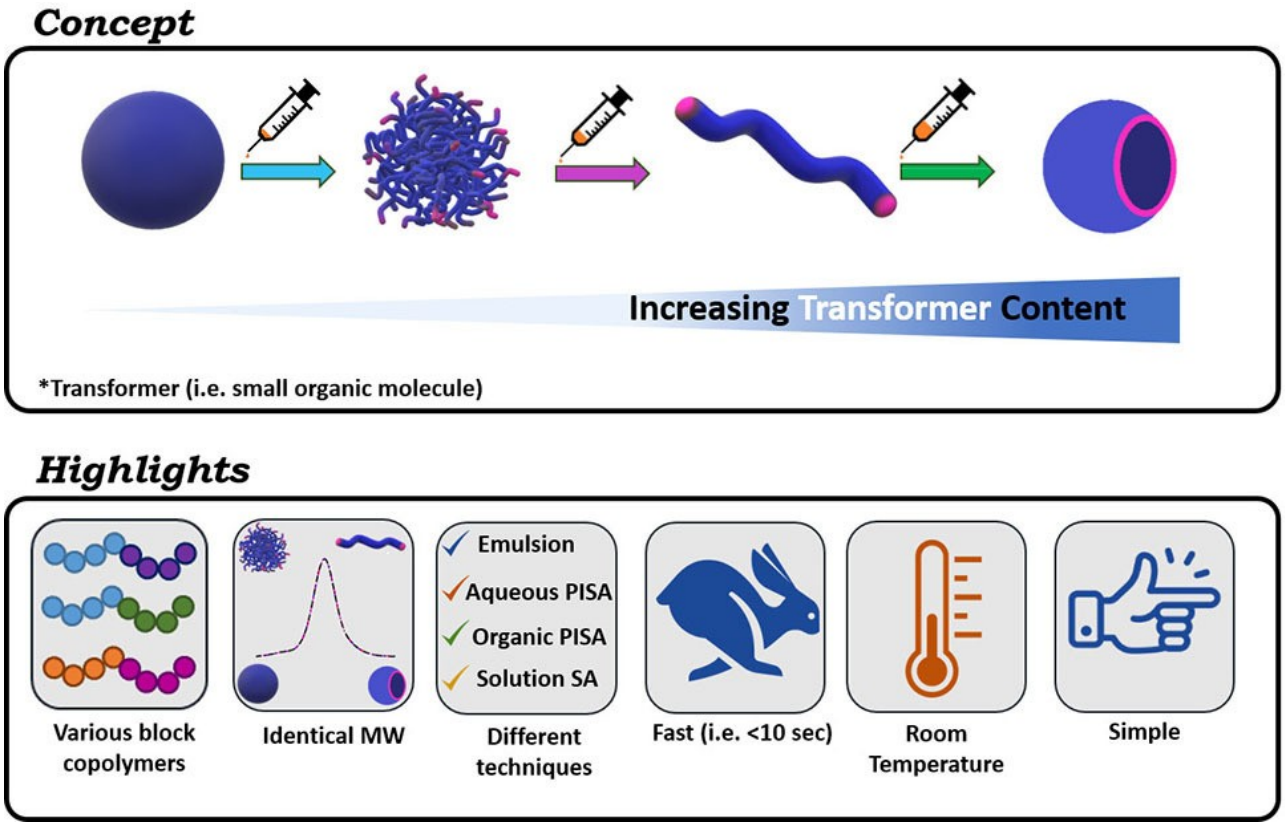

Figure 1. Schematic illustration and highlights of transformer-induced metamorphosis (TIM).

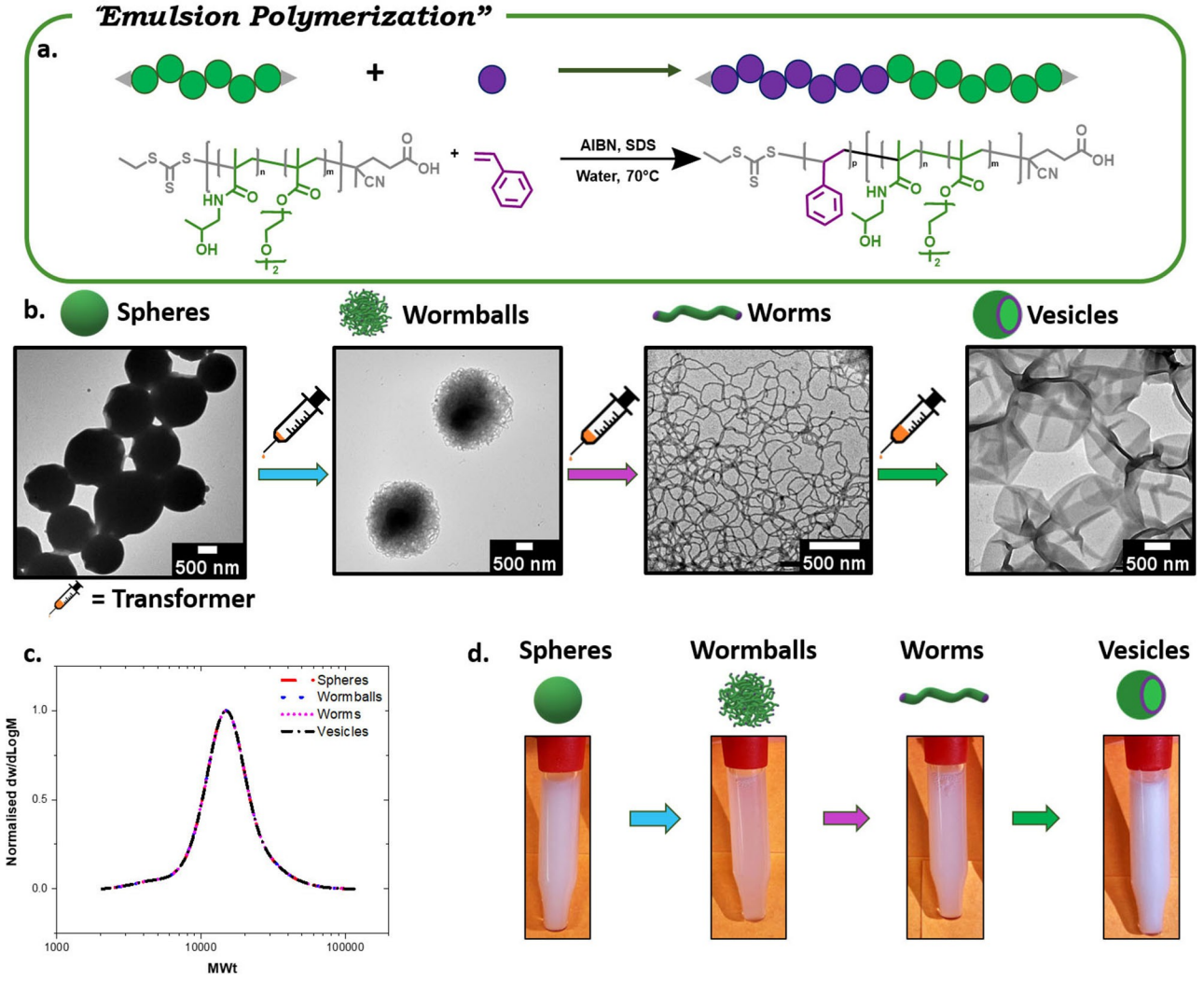

Figure 2. TIM of polymeric nanoparticles obtained via emulsion polymerization. a) Schematic representation of RAFT emulsion polymerization; b) TEM images of spheres, wormballs, worms and vesicles; c) SEC traces showing identical molecular weight distributions of various morphologies; d) Schematic representation of the morphologies and visualization of change in turbidity of P((DEGMA-*co*-HPMA)-*b*-styrene) nanoparticles in water after sequential addition of transformer.

solubility parameter similar to that of the core) does not only plasticize the PS core, thus increasing the mobility of the rigid PS chains, but also facilitates the morphological transformation. To confirm this hypothesis, we continued adding the transformer in the worm-like nanoparticles anticipating a switch to an even higher order morphology. As expected, the formation of vesicles was evident by TEM (additional 35 $\mu L\,mL^{-1}$) and was also supported by a change in turbidity (Figure 2d). This data suggest that toluene plays the role of a morphological transformer. In particular, toluene exhibits a very similar solubility parameter with that of the PS core (i.e. $\delta_{PS} = 16.6–20.2$, and $\delta_{toluene} = 18.2$) and therefore it can enter the core and increase the volume of the core hydrophobic segment (v).[17] Such change in v increases the critical packing parameter p ($p = v/al$), leading to the transformation into different morphologies.[18] Importantly, the ^{1}H NMR spectra of the polymers before and after the transformation showed identical chemical structures (Figure S6), thus confirming that the shape transformation occurred without altering the polymer composition. In addition, size exclusion chromatography (SEC) revealed indistinguishable molecular weight distributions for all the obtained nanoparticles (Figure 2c), which is in contrast to traditional PISA whereby the change in the molecular weight of the second block triggers the morphological transformation. Instead, in our approach, the addition of a small amount of transformer is solely responsible for the rapid evolution to the next higher-order morphology. It is noted that our strategy is different to many other techniques based on controlling either the self-assembly process or the interfacial interaction between the polymeric corona and the surrounding medium.[11c]

We were then interested in exploring whether the transformer-induced metamorphosis of polymeric nanoparticles could be applied not only to different block copolymers, but also to various self-assembly systems. To inves-

tigate this, an aqueous PISA formulation was followed utilizing poly(glycerol monomethacrylate) (PGMA) as the hydrophilic stabilizer block and poly(glycidyl methacrylate) (PGlyMA) as the core-forming block (Figures 3a and S7).

It is noted that this is a completely different diblock than in the previous system, in order to highlight the versatility of our method. In particular, in the emulsion approach the diblock was composed of a thermo-responsive corona and a hydrophobic PS core. Instead, in the current PISA example, the diblock consists of a water-soluble corona and PGlyMA as the core. By targeting a degree of polymerization (DP 35) of GlyMA, full monomer conversion was obtained and TEM analysis exclusively showed spherical nanoparticles (≈15 nm) (Figures 3b and S8).[19] GlyMA was then added as the molecular transformer as this would resemble the solubility parameter of the core. By injecting GlyMA (60 μL mL^{-1}), a rapid and quantitative transformation from spherical to worm-like nanoparticles was observed (Figure 3b).

The morphological change was also accompanied by the formation of a gel, as can be seen in Figure 3c, further supporting the formation of worm-like nanoparticles. Although this PISA system produced spherical micelles (which are different to the spherical aggregates formed by the emulsion approach), both systems can undergo a transformation from spheres to worms, thus being consistent with TIM. Upon adding more transformer, a fluid emulsion-like solution was generated and TEM confirmed the formation of vesicles. The morphology assignments were confirmed by small-angle X-ray scattering (SAXS) in solution. The

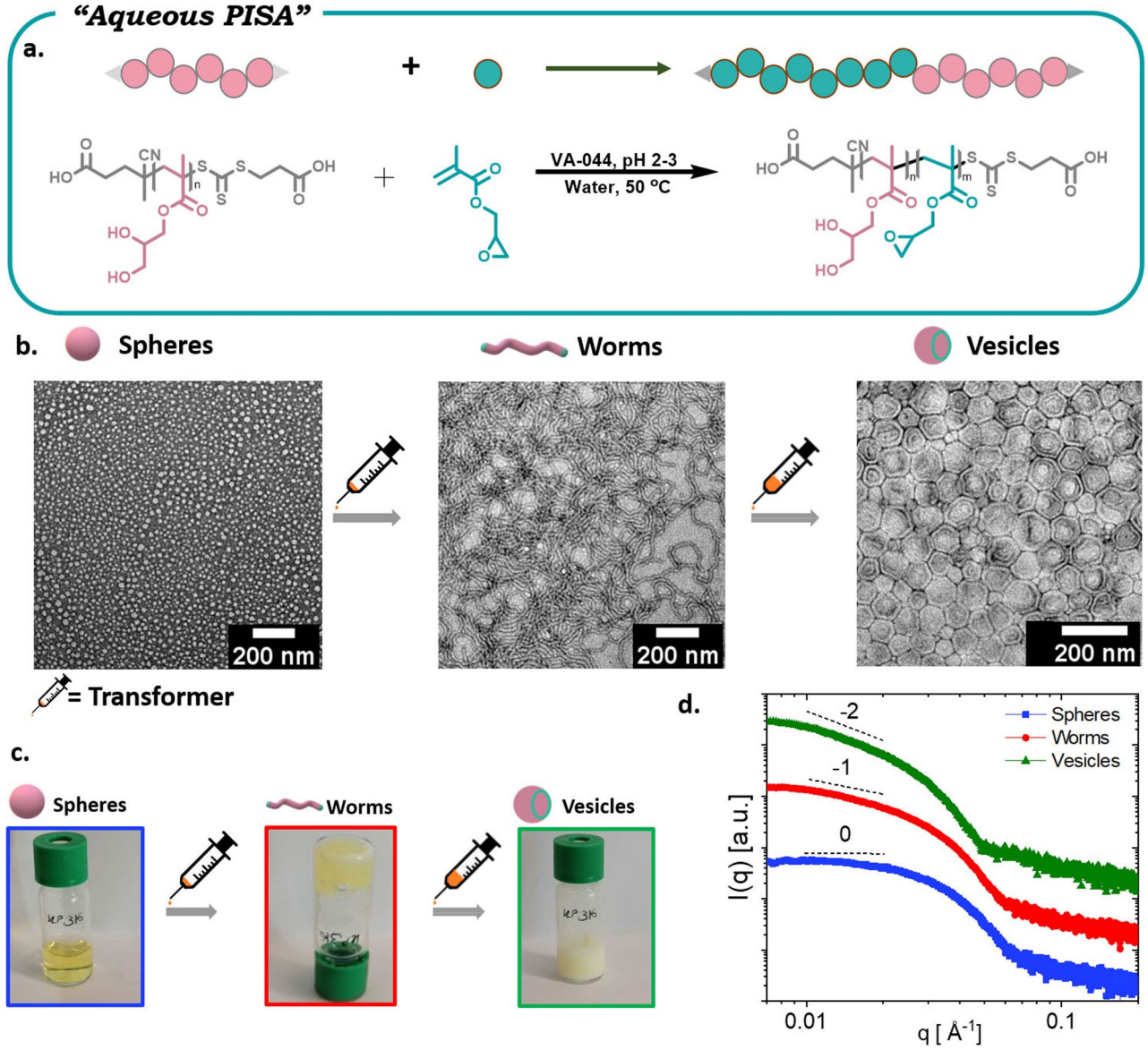

Figure 3. TIM of polymeric nanoparticles obtained via aqueous PISA. a) Schematic representation of RAFT emulsion polymerization; b) TEM images of spheres, worms and vesicles; c) visual representation of various morphologies; d) small-angle X-ray scattering data confirming the formation of different morphologies in bulk.

radially integrated SAXS patterns, shown as the intensity I as a function of the scattering vector q, are interpreted based on the slopes of form factors for monodisperse and dilute solutions (Figure 3d). A low-q slope of nearly 0 indicates spherical morphologies, while a slope of −1 indicates linear rigid morphologies, such as worms. Slopes of −2 are related to the presence of flat aggregates consistent with vesicles,[19] confirming that the morphologies assigned by TEM are in line with SAXS characterization. Last but not least, SEC analysis showed identical molecular weights for all the obtained morphologies (Figure S9). As such, it is evident that TIM of polymeric nanoparticles can operate efficiently in various systems, without the need to change the temperature or pH, which is distinct from recently reported approaches.[11c] To further probe the potential of our approach, an organic PISA formulation was subsequently employed.[20] Poly(oligo(ethylene glycol)) methyl ether methacrylate (POEGMA, average M_n 300) was used as the hydrophilic macromolecular chain transfer agent and the RAFT dispersion polymerization of styrene was conducted in methanol (Figures S10 and S11). After polymerization, the solution was dialyzed against water to remove methanol and unreacted monomer. The resulting solution was then analyzed by TEM and distinct worm-like nanoparticles were observed (Figure 4b). A small amount of toluene was then added (5 μL mL^{-1}) which induced the transformation from worms to vesicles. Cryogenic TEM further confirmed the existence of worms and vesicles in solution, thus supporting the successful morphological transformation (Figure 4c). This data also highlighted that the observed morphologies are not an artifact of a "drying" effect as in the solvent evaporation methodologies.[21] The transformation could

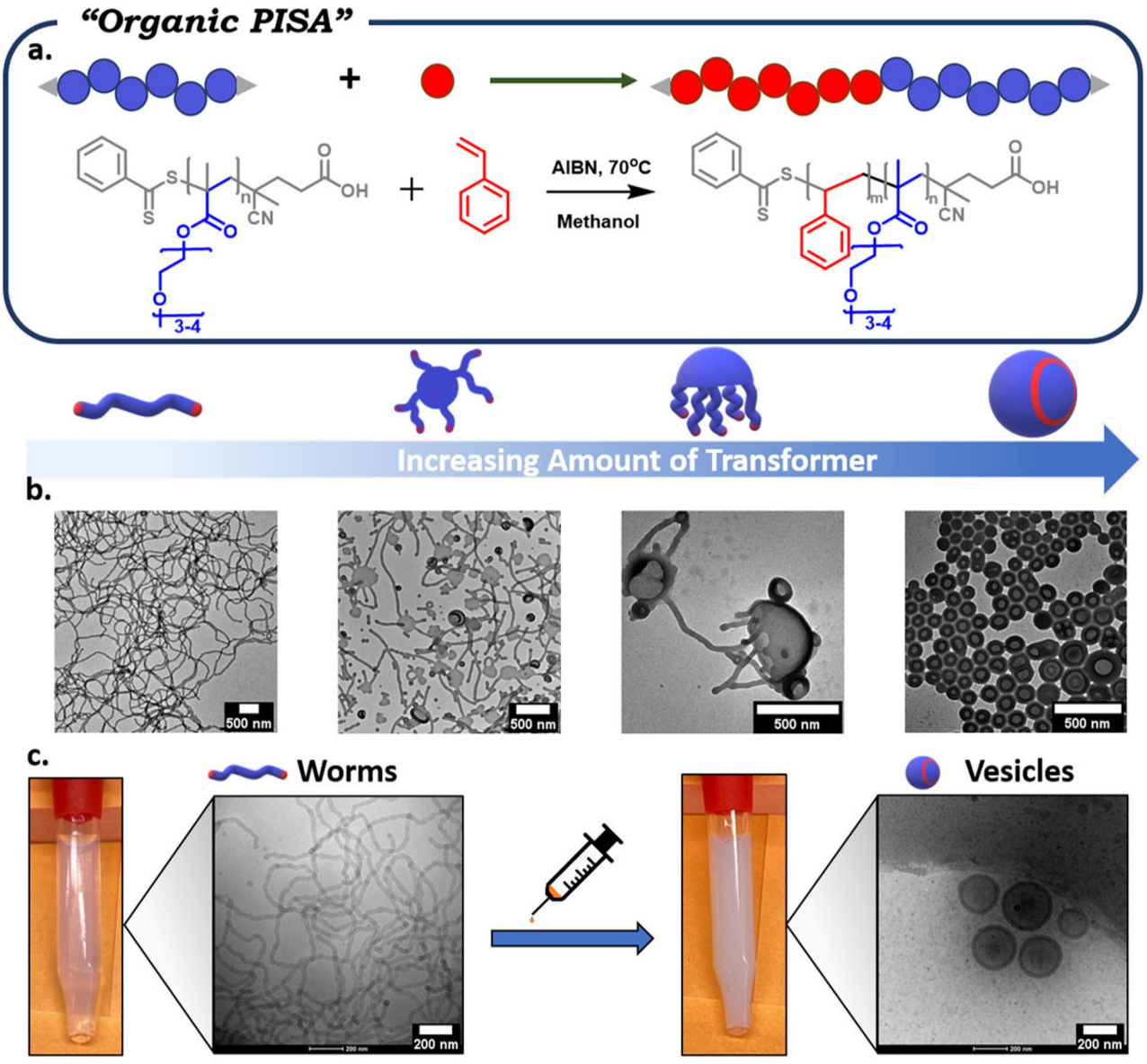

Figure 4. TIM of polymeric nanoparticles obtained via organic PISA. a) Schematic representation of RAFT dispersion polymerization; b) TEM images of worms, octopi-like morphology, jellyfish and vesicles respectively; c) visual representation and cryo-EM of worms and vesicles.

also be visualized by a clear change in turbidity. It is noted that SEC traces of both worms and vesicles showed overlapping molecular weight distributions (Figure S12). Interestingly, at even lower transformer concentrations (2 μL mL^{-1} and 3 μL mL^{-1}), several characteristic intermediate morphologies were observed. In particular, mixed phases consisting of flat lamellar disks interlinked with worms (octopi-like morphology) and jellyfish-like morphologies could be clearly detected by TEM. These intermediate morphologies not only suggest that we indeed have a transformation from worms to vesicles, but also indicate that the transformer is triggering a similar mechanistic pathway to traditional PISA but without the need to increase the molecular weight of the second block.[22] We also conducted additional experiments in which various organic molecules were used as potential morphological transformers. Interestingly, water-miscible organic molecules, such as tetrahydrofuran, could not alter the worm-like shape. In contrast, other water-immiscible molecules including styrene, xylene and mesitylene could act as efficient transformers owing to their resemblance with the hydrophobic core. Instead, cyclohexane and hexane, despite being water-immiscible, did not lead to a successful morphological transformation under the conditions studied. This may be due to their saturated structure which is different to the PS core (Figure S13). As a final experiment, the block copolymer obtained by organic PISA was freeze-dried and re-dissolved in acetone. A traditional self-assembly procedure in water was then followed and upon dialysis TEM showed the formation of worms. TIM was then applied by the addition of toluene and the shape was instantly changed from worms to vesicles (Figure S14). These preliminary data suggest that our method can also be applied in traditional self-assembly strategies.

In summary, we have developed a transformer-induced metamorphosis strategy that allows for the rapid transformation between different morphologies by adjusting the amount of an added organic molecule that matches the solubility parameter of the core. The successful transformation was confirmed by TEM, cryo-EM, and SAXS while SEC revealed identical molecular weights for all the obtained morphologies. Importantly, our approach operates at room temperature and without altering the chemical structure of the obtained morphologies. We envisage that such strategy can further enable structure-property relationship studies and theoretical simulations.

Acknowledgements

A.A. gratefully acknowledges ETH Zurich for financial support. N.P.T. acknowledges the award of a DECRA Fellowship and DP from the ARC (DE180100076 and DP200100231). K.P. thanks the Onassis Foundation, as this scientific paper was supported by the Onassis Foundation - Scholarship ID: FZQ051-1/2020-2021. We are grateful to ScopeM (ETH Zürich) and Monash Centre for Electron Microscopy, a Node of Microscopy Australia, for access to the electron microscopy facilities. Open access funding provided by Eidgenossische Technische Hochschule Zurich.

Conflict of Interest

The authors declare no conflict of interest.

Keywords: Block copolymers · Controlled radical polymerization · Solution polymer self-assembly

[1] F. Gomollón-Bel, *Chem. Int.* **2019**, *41*, 12–17.
[2] a) K. Parkatzidis, H. S. Wang, N. P. Truong, A. Anastasaki, *Chem* **2020**, *6*, 1575–1588; b) N. Corrigan, K. Jung, G. Moad, C. J. Hawker, K. Matyjaszewski, C. Boyer, *Prog. Polym. Sci.* **2020**, *111*, 101311; c) K. Matyjaszewski, N. V. Tsarevsky, *Nat. Chem.* **2009**, *1*, 276–288; d) N. Zaquen, M. Rubens, N. Corrigan, J. Xu, P. B. Zetterlund, C. Boyer, T. Junkers, *Prog. Polym. Sci.* **2020**, *107*, 101256; e) C. Barner-Kowollik, *Handbook of RAFT polymerization*, Wiley, Hoboken, **2008**; f) N. P. Truong, G. R. Jones, K. G. E. Bradford, D. Konkolewicz, A. Anastasaki, *Nat. Chem. Rev.* **2021**, *5*, 859–869.
[3] a) Y. Mai, A. Eisenberg, *Chem. Soc. Rev.* **2012**, *41*, 5969–5985; b) N. J. Warren, S. P. Armes, *J. Am. Chem. Soc.* **2014**, *136*, 10174–10185.
[4] F. d′Agosto, J. Rieger, M. Lansalot, *Angew. Chem. Int. Ed.* **2020**, *59*, 8368–8392; *Angew. Chem.* **2020**, *132*, 8444–8470.
[5] L. Zhang, A. Eisenberg, *J. Am. Chem. Soc.* **1996**, *118*, 3168–3181.
[6] C. Liu, C.-Y. Hong, C.-Y. Pan, *Polym. Chem.* **2020**, *11*, 3673–3689.
[7] a) S. Ganda, M. H. Stenzel, *Prog. Polym. Sci.* **2020**, *101*, 101195; b) J. M. Ren, A. S. Knight, B. G. van Ravensteijn, P. Kohl, R. Bou Zerdan, Y. Li, D. J. Lunn, A. Abdilla, G. G. Qiao, C. J. Hawker, *J. Am. Chem. Soc.* **2019**, *141*, 2630–2635; c) A. M. Oliver, J. Gwyther, C. E. Boott, S. Davis, S. Pearce, I. Manners, *J. Am. Chem. Soc.* **2018**, *140*, 18104–18114.
[8] N. P. Truong, M. R. Whittaker, C. W. Mak, T. P. Davis, *Expert Opin. Drug Delivery* **2015**, *12*, 129–142.
[9] a) N. P. Truong, J. F. Quinn, M. R. Whittaker, T. P. Davis, *Polym. Chem.* **2016**, *7*, 4295–4312; b) Y. Geng, P. Dalhaimer, S. Cai, R. Tsai, M. Tewari, T. Minko, D. E. Discher, *Nat. Nanotechnol.* **2007**, *2*, 249–255; c) J. Tan, H. Sun, M. Yu, B. S. Sumerlin, L. Zhang, *ACS Macro Lett.* **2015**, *4*, 1249–1253; d) B. Karagoz, L. Esser, H. T. Duong, J. S. Basuki, C. Boyer, T. P. Davis, *Polym. Chem.* **2014**, *5*, 350–355.
[10] a) S. Kaga, N. P. Truong, L. Esser, D. Senyschyn, A. Sanyal, R. Sanyal, J. F. Quinn, T. P. Davis, L. M. Kaminskas, M. R. Whittaker, *Biomacromolecules* **2017**, *18*, 3963–3970; b) M. N. Vu, H. G. Kelly, A. K. Wheatley, S. Peng, E. H. Pilkington, N. A. Veldhuis, T. P. Davis, S. J. Kent, N. P. Truong, *Small* **2020**, *16*, 2002861.
[11] a) L. Zhang, K. Yu, A. Eisenberg, *Science* **1996**, *272*, 1777–1779; b) D. S. Achilleos, T. A. Hatton, M. Vamvakaki, *J. Am. Chem. Soc.* **2012**, *134*, 5726–5729; c) Y. Pei, A. B. Lowe, P. J. Roth, *Macromol. Rapid Commun.* **2017**, *38*, 1600528; d) C. L. McCormick, B. S. Sumerlin, B. S. Lokitz, J. E. Stempka, *Soft Matter* **2008**, *4*, 1760–1773; e) M. Rolland, N. P. Truong, K. Parkatzidis, E. H. Pilkington, A. L. Torzynski, R. W. Style, E. R. Dufresne, A. Anastasaki, *JACS Au* **2021**, https://doi.org/doi.org/10.1021/jacsau.1c00321.
[12] L. A. Fielding, J. A. Lane, M. J. Derry, O. O. Mykhaylyk, S. P. Armes, *J. Am. Chem. Soc.* **2014**, *136*, 5790–5798.

[13] a) L. P. Ratcliffe, M. J. Derry, A. Ianiro, R. Tuinier, S. P. Armes, *Angew. Chem. Int. Ed.* **2019**, *58*, 18964–18970; *Angew. Chem.* **2019**, *131*, 19140–19146; b) C. A. Figg, A. Simula, K. A. Gebre, B. S. Tucker, D. M. Haddleton, B. S. Sumerlin, *Chem. Sci.* **2015**, *6*, 1230–1236.
[14] a) L. Li, S. Cui, A. Hu, W. Zhang, Y. Li, N. Zhou, Z. Zhang, X. Zhu, *Chem. Commun.* **2020**, *56*, 6237–6240; b) J. R. Lovett, N. J. Warren, L. P. Ratcliffe, M. K. Kocik, S. P. Armes, *Angew. Chem. Int. Ed.* **2015**, *54*, 1279–1283; *Angew. Chem.* **2015**, *127*, 1295–1299; c) L. P. Ratcliffe, C. Couchon, S. P. Armes, J. M. Paulusse, *Biomacromolecules* **2016**, *17*, 2277–2283.
[15] a) W. Zhang, C. Gao, *J. Mater. Chem. A* **2017**, *5*, 16059–16104; b) H. Phan, V. Taresco, J. Penelle, B. Couturaud, *Biomater. Sci.* **2021**, *9*, 38; c) S. J. Byard, C. T. O'brien, M. J. Derry, M. Williams, O. O. Mykhaylyk, A. Blanazs, S. P. Armes, *Chem. Sci.* **2020**, *11*, 396–402.
[16] N. P. Truong, M. R. Whittaker, A. Anastasaki, D. M. Haddleton, J. F. Quinn, T. P. Davis, *Polym. Chem.* **2016**, *7*, 430–440.
[17] A. F. Barton, *Chem. Rev.* **1975**, *75*, 731–753.
[18] C. A. Figg, R. N. Carmean, K. C. Bentz, S. Mukherjee, D. A. Savin, B. S. Sumerlin, *Macromolecules* **2017**, *50*, 935–943.
[19] F. L. Hatton, M. J. Derry, S. P. Armes, *Polym. Chem.* **2020**, *11*, 6343–6355.
[20] L. Esser, N. P. Truong, B. Karagoz, B. A. Moffat, C. Boyer, J. F. Quinn, M. R. Whittaker, T. P. Davis, *Polym. Chem.* **2016**, *7*, 7325–7337.
[21] a) D. J. Pochan, Z. Chen, H. Cui, K. Hales, K. Qi, K. L. Wooley, *Science* **2004**, *306*, 94–97; b) J. J. Shin, E. J. Kim, K. H. Ku, Y. J. Lee, C. J. Hawker, B. J. Kim, *ACS Macro Lett.* **2020**, *9*, 306–317.
[22] A. Blanazs, J. Madsen, G. Battaglia, A. J. Ryan, S. P. Armes, *J. Am. Chem. Soc.* **2011**, *133*, 16581–16587.

Manuscript received: October 15, 2021
Version of record online: January 11, 2022